Relationships between *in vivo* microdamage and the remarkable regional material and strain heterogeneity of cortical bone of adult deer, elk, sheep and horse calcanei

John G. Skedros,[1,2] Christian L. Sybrowsky,[2] Wm. Erick Anderson[2] and Frank Chow[2]

[1]*Department of Orthopaedic Surgery, University of Utah and the Utah Bone and Joint Center, Salt Lake City, UT, USA*
[2]*Department of Veteran's Affairs Medical Center, Bone and Joint Research Laboratory, Salt Lake City, UT, USA*

Abstract

Natural loading of the calcanei of deer, elk, sheep and horses produces marked regional differences in prevalent/predominant strain modes: compression in the dorsal cortex, shear in medial–lateral cortices, and tension/shear in the plantar cortex. This consistent non-uniform strain distribution is useful for investigating mechanisms that mediate the development of the remarkable regional material variations of these bones (e.g. collagen orientation, mineralization, remodeling rates and secondary osteon morphotypes, size and population density). Regional differences in strain-mode-specific microdamage prevalence and/or morphology might evoke and sustain the remodeling that produces this material heterogeneity in accordance with local strain characteristics. Adult calcanei from 11 animals of each species (deer, elk, sheep and horses) were transversely sectioned and examined using light and confocal microscopy. With light microscopy, 20 linear microcracks were identified (deer: 10; elk: six; horse: four; sheep: none), and with confocal microscopy substantially more microdamage with typically non-linear morphology was identified (deer: 45; elk: 24; horse: 15; sheep: none). No clear regional patterns of strain-mode-specific microdamage were found in the three species with microdamage. In these species, the highest overall concentrations occurred in the plantar cortex. This might reflect increased susceptibility of microdamage in habitual tension/shear. Absence of detectable microdamage in sheep calcanei may represent the (presumably) relatively greater physical activity of deer, elk and horses. Absence of differences in microdamage prevalence/morphology between dorsal, medial and lateral cortices of these bones, and the general absence of spatial patterns of strain-mode-specific microdamage, might reflect the prior emergence of non-uniform osteon-mediated adaptations that reduce deleterious concentrations of microdamage by the adult stage of bone development.

Key words: bone histomorphometry; bone remodeling; deer calcanei; elk calcanei; horse calcanei; mechanical loading; microdamage; sheep calcanei.

Introduction

In vivo strain measurements from limb bones of various mammalian species show that many[1] are typically loaded in directionally consistent bending during controlled ambulation, which produces a habitual distribution of prevalent/predominant tension, compression and shear strains in regions that are quasi-mutually exclusive (Biewener & Bertram, 1993; Lanyon et al. 1979; Fritton & Rubin, 2001; Lieberman et al. 2003; Moreno et al. 2008). Experimental studies have also demonstrated that the morphology and incidence of matrix microdamage in fatigue- and monotonically loaded bone are highly dependent on these strain modes (Boyce et al. 1998; Reilly & Currey, 1999; Colopy et al. 2004; George & Vashishth, 2005; Robling et al. 2006; Wang & Niebur, 2006; Ebacher et al. 2007). Consequently, many bones are faced with the dilemma of incurring microdamage as a potentially deleterious byproduct of non-uniform strain distributions.

Experimental studies that have provided insight into how bones might adapt to avoid or accommodate microdamage have often focused on *ex vivo* loading tests of machined bone specimens (Martin et al. 1998; Currey, 2002; Donahue

& Galley, 2006). The prevalence and morphology of *in vivo* microdamage in whole bones from natural conditions (i.e. not subjected to fatigue or monotonic testing) have been relatively understudied, especially in wild animals. Experimental studies by Reilly and co-workers (Reilly & Currey, 1999; Reilly, 2000) of bovine, equine and human bone have shown that cortical bone microdamage can occur, albeit at low levels, during physiological loading that does not exceed yield strains. Skedros et al. (2003) also found few microcracks in bones of adult wild deer that were evaluated using light microscopy (rib, humerus, radius, principal metacarpal and proximal phalanx). It is possible that the paucity of microdamage in natural conditions is correlated with the ability of bone to accommodate microdamage by 'toughening' a cortical region through histomorphological features, such as secondary osteon interfaces (e.g. cement lines and interlamellar seams) or variations in predominant collagen fiber orientation, which can decrease microdamage propagation and enable their efficient repair (Reilly et al. 1997; Hiller et al. 2003; Vashishth, 2004;Gibson et al. 2006). This hypothesis is supported by studies suggesting that although secondary osteonal bone is poor at minimizing microcrack formation, it is proficient at attenuating the distance and rate of microcrack propagation (Reilly et al. 1997; Martin et al. 1998; Reilly & Currey, 1999; O'Brien et al. 2003). In turn, the formation of microdamage, as long as it is not excessive, can absorb energy that might otherwise lead to fracture (Reilly et al. 1997; Donahue et al. 2000; Donahue & Galley, 2006). Consequently, in adult limb bones that naturally experience habitual bending, there may be regional disparities in 'beneficial' microdamage prevalence and morphology that are associated with regional microstructural differences (Martin, 2007; Kennedy et al. 2008).

Artiodactyl (e.g. sheep and deer) and perissodactyl (horse) calcanei have been described as relatively simply and habitually loaded 'tension∕compression' bones (Skedros et al. 1994, 1997; Su et al. 1999; Fig. 1). *In vivo* and rigorous *ex vivo* (with up to seven stacked-rosette strain gages on the bone, including on the plantar cortex) studies have shown that during physiological weight-bearing activities, the artiodactyl calcaneal diaphysis behaves like a short-cantilevered beam, with longitudinal compression and tension strains predominating on opposing dorsal and plantar cortices, respectively (Lanyon, 1974; Su et al. 1999). Unpublished data show that this strain distribution is highly consistent, even with extremes of off-axis loading simulating darting and turning during ambulation (Su, 1998). These experimental results demonstrate that during > 80% of stance phase there is a highly consistent distribution of: (i) net compression in the dorsal cortex and net tension in the plantar cortex; and (ii) shear strains in the plantar cortex and neutral axis regions (Su et al. 1999). By the adult stage, the material variations between cortical regions within the same transverse cross-section of these bones are the most dramatic that have been described in any other vertebrates. For example, when compared with
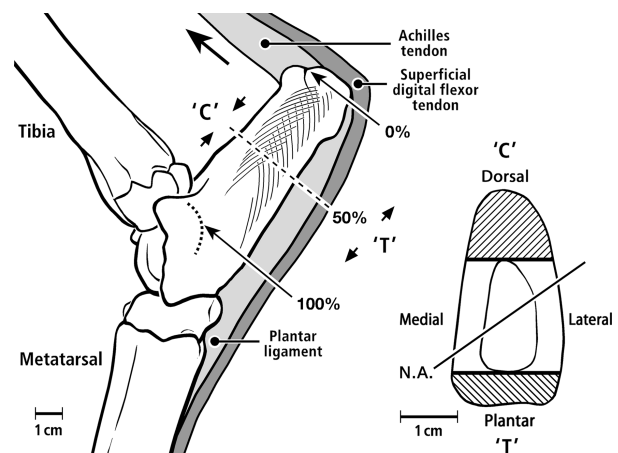
Fig. 1 Lateral view of a calcaneus of an adult mule deer showing associated bones, ligaments and tendons. The cross-section shows the neutral axis (N.A.), the location of which was estimated in an *ex vivo* study using four rosette strain gages at the same cross-section (Su et al. 1999). It is speculated that the neutral axis is similarly oblique in the other calcanei. Also shown are the dorsal, plantar, medial and lateral cortical locations where the analyses were performed, with oblique lines distinguishing these main areas. 'C' and 'T' indicate that these cortices receive predominant compression or tension, respectively. *Ex vivo* analyses have also shown that shear strains are prevalent across the section, dominating in the medial and lateral cortices, and with relatively high levels in the plantar cortex. The distance from 0 to 100% represents what we have previously defined as the biomechanical shaft 'length', with 0% representing the distal end of the shaft and 100% representing the central aspect of the articular surface.

the other cortical regions, the plantar 'tension∕shear' cortex has lower overall mineralization, greater mineralization heterogeneity, more longitudinally oriented collagen fibers and more 'hooped' secondary osteon morphotypes (Skedros et al. 1994, 2001, 2004, 2006b, 2007, 2009). It is not known if this remarkable regional material heterogeneity represents osteon-mediated adaptive responses to a history or ongoing production of regional differences of microdamage morphology and∕or prevalence.

The purpose of this study is to examine cross-sections of adult sheep, deer, elk and horse calcanei for the distribution and morphology of *in vivo* 'natural' microdamage in cortical regions representing their highly non-uniform strain environments. We hypothesized that the distribution and morphology of microdamage will differ between dorsal, plantar, medial and lateral cortices in accordance with their prevalent∕predominant strain differences: (i) short transverse linear microcracks and debonded secondary osteons in a habitual tension environment (plantar cortex); (ii) relatively longer and more numerous linear∕longitudinal microcracks in a habitual compression environment (dorsal cortex); (iii) complex∕multiplanar microdamage entities in shear environments (medial and lateral cortices = neutral axis); and (iv) diverse microdamage morphologies (e.g. wispy, diffuse and complex linear) in 'tension∕shear' environments (plantar

cortex, and also likely in the neutral axis; Boyce et al. 1998; Reilly & Currey, 1999; George & Vashishth, 2005). Additionally, to estimate regional differences in remodeling activity, which might correlate with microdamage morphology, prevalence and/or the effectiveness of their repair, new remodeling events (NREs; population densities of resorption spaces and newly forming secondary osteons) were also quantified.

Materials and methods

### Strain data for the artiodactyl/perissodactyl calcaneus models

The *in vivo* strain data obtained by Lanyon (1973, 1974) are from varying lateral locations of domesticated sheep calcanei. The data in deer calcanei are *ex vivo*, and were obtained from bones that were loaded in a fixed position simulating mid-stance (Su et al. 1999). There are no *in vivo* or *ex vivo* strain data for the horse and elk calcanei. These limitations are elaborated upon in the Discussion.

Specimens and specimen preparation

The left calcaneus from each of 11 wild Rocky Mountain mule deer, 11 wild North American elk, 11 domesticated horses (mixed breeds) and 11 domesticated sheep were obtained from adult animals with no evidence of skeletal pathology or advanced age (i.e. based on antler morphology and/or dental wear). The use of these animals was approved by the Institutional Animal Care and Utilization Committee (IACUC) at the University of Utah (for the Orthopaedic Bioengineering Research Laboratory). The mule deer (*Odocoileus hemionus hemionus*) and elk (*Cervus elaphus*) were wild males that were shot in Utah (USA) in their natural habitat during October hunting seasons. The deer and elk were 3–4 years old, which is mature but not elderly in these species. At the time of collection, the periosteal ('velvet') covering of the antlers had been shed and antler growth was complete, suggesting that the relatively minor amount of appendicular cortical bone that had been resorbed for antler growth would have been replenished by this stage (Banks et al. 1968; Hillman et al. 1973). Calcanei from sheep (*Ovis aries*; 2 years old; breed is crossed Suffolk/Hampshire and Rambouillet) and horses (2–9 years old) were obtained from animals that were killed for reasons other than limb lameness or any other skeletal-related illness, and no animals were specifically killed for this study. The specific ages of the horses were uncertain because the carcasses had been taken to a regional abattoir where identification of the individual animals was not possible at the time of specimen collection. None of the horses had a history of racing or race training.

Using a diamond blade saw (Exact Technologies, Oklahoma City, OK, USA) and continuous water irrigation, one 12–14-mm-thick transverse section was cut from each calcaneus between 50% and 80% of shaft length (Fig. 2). These sections were bulk stained in 1% basic fuchsin in absolute ethanol (Burr & Stafford, 1990; Burr & Hooser, 1995). Due to thicker cortices of the bones used in the present study, the infiltration time for dye penetration was increased to 96 total hours.

Subsequent to staining, three 125-μm-thick sections were cut transversely from the middle portion of the larger bulk-stained
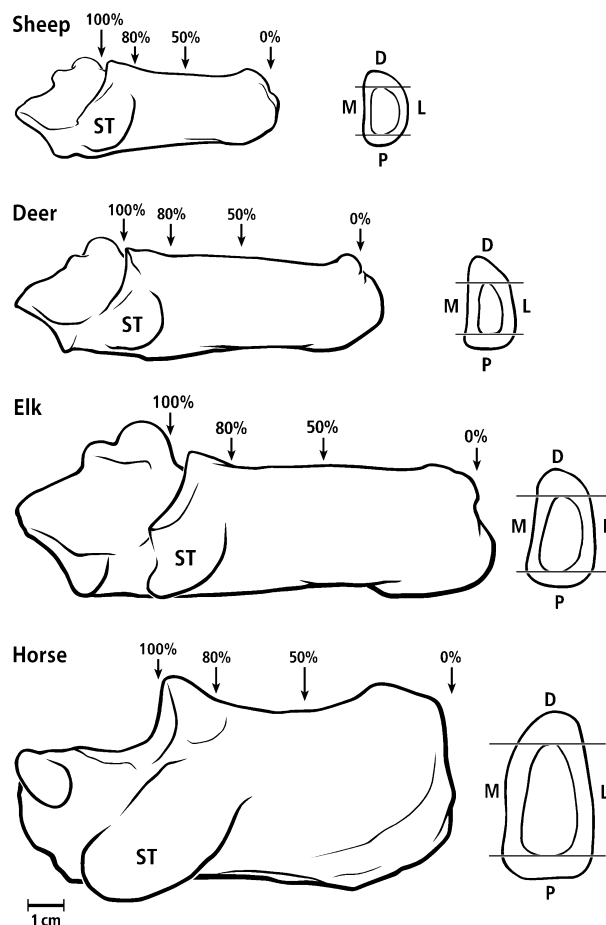
Fig. 2 Medial views of sheep, deer, elk and horse calcanei. At the right are cross-sections showing the dorsal (D), plantar (P), medial (M) and lateral (L) cortical locations where the analyses were performed. The distance from 0 to 100% represents what we have previously defined as the biomechanical shaft 'length', with 0% representing the distal end of the shaft and 100% representing the central aspect of the articular surface. ST, sustentaculum talus.

sections. Because kerf loss of the saw blade is 0.3 mm, it is unlikely that the same microcrack would be observed in two sections (Taylor & Lee, 1998; Donahue et al. 2000). These thin, unembedded, sections ($n = 3$ per bone) were ground (600 grit paper) and buffed on a lapidary wheel to an overall thickness of 100 μm, and mounted with microscope immersion oil (to enhance resolution) onto glass slides for examination under the microscope.

Light microscopy

The entire cortical areas of the three fuchsin-dyed slices from each bone (33 slices from each species; 132 total slices) were thoroughly examined by two trained investigators (CS; FC) who worked independently, and were blinded to the objectives and hypotheses of the study. Using the light microscope, these investigators counted resorption spaces and newly forming secondary osteons, and counted and recorded the locations of *in vivo* microcracks on a stereological grid superimposed on enlarged tracings of the sections. Resorption spaces are defined as void

spaces having crenulated margins with no light-microscopic evidence of mineralized bone within the resorption space. Newly forming secondary osteons are defined as those osteons with less than half of their radial closure with mineralized bone in two or more quadrants (Skedros et al. 2004). To ensure that the microcracks seen in our bone specimens were consistent with microcracks described by previous investigators (Lee et al. 1998; Donahue et al. 2000), we examined *in vivo* and artifactual microcracks in several thin slices used by Burr and Stafford (1990; provided by D.B. Burr). Potential microcracks were examined at 62.5–400 ×.

In addition to exhibiting a distinct increase of fuchsin staining along its margins (Frost, 1960; Burr & Stafford, 1990), each putative microcrack was included in the final data set only if a consensus for inclusion was also reached. This final selection process also included an independent examination of all putative microdamage entities by the principal investigator (JS), who was blinded to species and cortical location.

Using a video camera and monitor (Sony Video Camera Model DXC-750MD; Sony Trinitron Color Video Monitor Model PVM-1343MD, Japan) interfaced to an image analysis system (Image 1; Universal Imaging, West Chester, PA, USA), 62.5 × microscopic fields containing linear-type microcracks were digitized for subsequent quantification of microcrack length. Areas of the cortical locations (dorsal, plantar, medial and lateral) were determined using scanned tracings of each bone section.

Confocal microscopy

Confocal microscopy was used because of its greater sensitivity for detecting non-linear forms of microdamage (Boyce et al. 1998; Vashishth et al. 2000), and to verify the presence of microdamage found using light microscopy (Diab & Vashishth, 2007). The entire cortical areas of all sections were examined for microdamage using confocal microscopy (Nikon PCM-2000, Melville, NY, USA) with a green HeNe laser (543 nm wavelength excitation) and a 565 long-pass emission filter (CY3/TR). Sections were viewed at 10 × (1.16 × 1.16 mm) to 400 × (Nikon Eclipse Microscope, E800).

All sections were thoroughly examined by two trained investigators (CS; WA) who worked independently, and were blinded to the objectives and hypotheses of the study. Expected microdamage morphologies included: (i) linear (as described above; Burr & Stafford, 1990; George & Vashishth, 2005); (ii) debonded, which are seen as subtle canalicular disruptions, and are typically near secondary osteons (Da Costa Gómez et al. 2005; Hazenberg et al. 2006); (iii) wispy (Boyce et al. 1998); (iv) diffuse (Boyce et al. 1998); and (v) complex/multiplanar (George & Vashishth, 2005). All other entities that might be manifestations of *in vivo* microdamage were also recorded on enlarged drawings. All possible forms of microdamage were viewed through the full thickness of the section to determine if they were consistent with the forms of microdamage described by previous investigators (Zioupos & Currey, 1994; Boyce et al. 1998; Lee et al. 1998; Reilly & Currey, 1999; Donahue et al. 2000; Da Costa Gómez et al. 2005; George & Vashishth, 2005).

Final microdamage inclusion by consensus

Following light and confocal microscopy, each microdamage entity was included only if a consensus was reached (JS; CS;

WA). This final selection process also included an independent examination of all putative microdamage entities by the principal investigator, who was blinded to species and cortical location. In the consensus process approximately 50% of microcracks were discarded, primarily because under polarized light they appeared to have adjacent bone matrix patterns typical of vascular structures. Microcracks produced by sectioning and tissue processing did not have fuchsin staining, and therefore were not counted. Because information about microcrack initiation, propagation and arrest can be inferred from local histomorphological features (Norman & Wang, 1997; Donahue et al. 2000), detailed drawings were made of the local microstructure surrounding each microdamage entity, including: mature secondary osteons; osteon cement lines; primary and secondary interstitial bone; newly forming secondary osteons; resorption spaces; primary osteons; and vascular spaces.

Statistical analysis

In order to identify statistical differences in NREs and the microdamage parameters, a three-factor analysis of variance (ANOVA) was conducted using species, cortical region (dorsal, plantar, medial, lateral) and section ($n = 3$ per bone). Age was not used as a covariate primarily because the age range was only known for the horses, and all other animals within each of the other species were of similar age. Differences between cortical regions within each species were then assessed for statistical significance using a Kruskal–Wallis multiple-comparison Z-test (Sokal & Rohlf, 1995; Number Cruncher Statistical Systems, 2004 version; J. Hintze, Kaysville, UT, USA). An alpha level of ≤ 0.01 was considered statistically significant for paired comparisons, and this represented a correction for multiple comparisons. Spearman correlation coefficients (r values) were determined for comparisons between microdamage prevalence and NREs.

Results

There are significant effects of species on the density of NREs and overall microdamage (includes all sizes, lengths and types of microdamage; no. per mm^2). *Post hoc* analysis of NRE data showed significant differences ($P \leq 0.01$) in the density of NREs between the deer, elk, equine and sheep calcanei in most comparisons (deer 0.156 mm^{-2}; elk 0.234 mm^{-2}; horse 0.144 mm^{-2}; sheep 0.385 mm^{-2}), except between elk and deer ($P = 0.7$). Excluding sheep calcanei (where no microdamage was found), analysis of microdamage density data showed significant differences ($P \leq 0.03$) in the density of microdamage between the deer, elk and equine calcanei in all possible comparisons (deer 0.017 mm^{-2}; elk 0.007 mm^{-2}; horse 0.002 mm^{-2}). Within each species, there were no significant effects of section ($n = 3$/bone) on overall microdamage density and NREs.

As shown in Table 1 and Fig. 3, significant differences ($P \leq 0.01$) were found between cortical regions for NRE density for each species and for overall microdamage density in the cortical regions of deer, elk and equine calcanei.

Table 1 Microdamage*.

	Total number (density, no. per mm^2)				
	Dorsal 'compression'	Plantar 'tension'	Medial	Lateral	All cortices
Deer					
Light microscopy					
Linear	–^{P}	8 (0.011)^{D,M,L}	2 (0.002)^P	–^{P}	10 (0.003)
Confocal microscopy					
Debonded	12 (0.008)^P	20 (0.028)^{D,M,L}	9 (0.011)^P	–^{P}	41 (0.012)
Wispy	–	1 (0.002)	–	–	1 (0.001)
Diffuse	–	3 (0.005)	–	–	3 (0.001)
Total	12 (0.008)	32 (0.046)	11 (0.013)	–	55 (0.017)
Elk					
Light microscopy					
Linear	–	6 (0.008)	–	–	6 (0.002)
Confocal microscopy					
Debonded	6 (0.003)^P	14 (0.016)^{D,M,L}	3 (0.002)^P	–^{P}	23 (0.005)
Wispy	–	–	–	–	–
Diffuse	–	1 (0.001)	–	–	1 (0.000)
Total	6 (0.003)	21 (0.025)	3 (0.002)	–	30 (0.007)
Horse					
Light microscopy					
Linear	1 (0.000)	1 (0.001)	1 (0.000)	1 (0.000)	4 (0.000)
Confocal microscopy					
Debonded	5 (0.001)	8 (0.003)^{M,L}	1 (0.000)^P	1 (0.000)^P	15 (0.001)
Wispy	–	–	–	–	–
Diffuse	–	–	–	–	–
Total	6 (0.001)	9 (0.004)	2 (0.001)	2 (0.001)	19 (0.002)

Data shown represent: total number of microdamage entities (microdamage density, no. per mm^2). Significantly different ($P < 0.01$) from cortical region indicated by superscripted letter. D, dorsal; L, lateral; M, medial; P, plantar.
*No microdamage was found in the specimens from sheep.
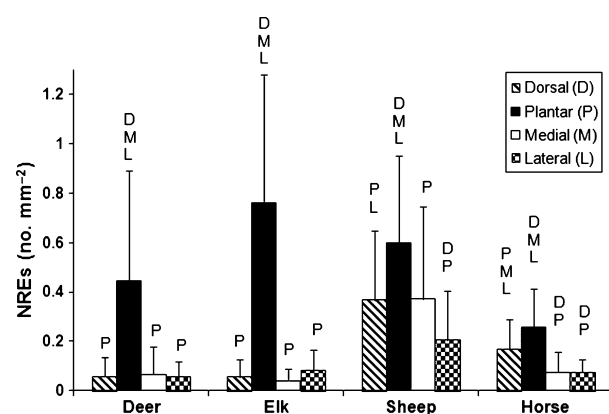
Fig. 3 Bar graphs of new remodeling events (NREs; no. per mm^2) in dorsal, plantar, medial and lateral cortices. NREs = resorption spaces plus newly forming secondary osteons. Significant differences ($P \leq 0.01$) between cortical regions are indicated for each region by using the letter that corresponds to the region that is significantly different: D, dorsal; P, plantar; M, medial; L, lateral. Error bars represent standard deviations.

NREs

In all species, the plantar 'tension/shear' cortex exhibited the greatest density of NREs, which was statistically greater than all other cortices ($P < 0.0001$ in deer and elk; $P < 0.01$ in horse and sheep; Fig. 3). This was most prominent in the wild animals (deer and elk), which showed substantially greater concentrations of NREs in the plantar cortex than in the dorsal cortex (7.7–14.1 times higher in deer and elk, respectively, vs. 1.5–1.6 times higher in sheep and horses, respectively). Correlation analyses showed little if any relationship between NREs and the prevalence of total microdamage (deer $r = 0.28$, $P < 0.01$; elk $r = 0.25$, $P < 0.01$; horses $r = 0.10$, $P = 0.3$).

Light microscopy: linear microcracks

Using light microscopy, a total of 20 linear microcracks were identified in the 132 sections (i.e. all bones in all four species; Table 1; Figs 4 and 5). Of the 20 microcracks observed, 10 were found in the deer (four bones), six in the elk (two bones) and four in the horse (three bones). No linear microcracks were observed in the sheep calcanei. Microcrack lengths ranged from 31.7 to 106.2 μm (mean: 52.0 μm). Representative microcracks viewed in the light microscope are shown in Fig. 5. Only two microcracks did not touch or enter a secondary osteon or cement line, but all microcracks were within 100 μm of a secondary osteon.
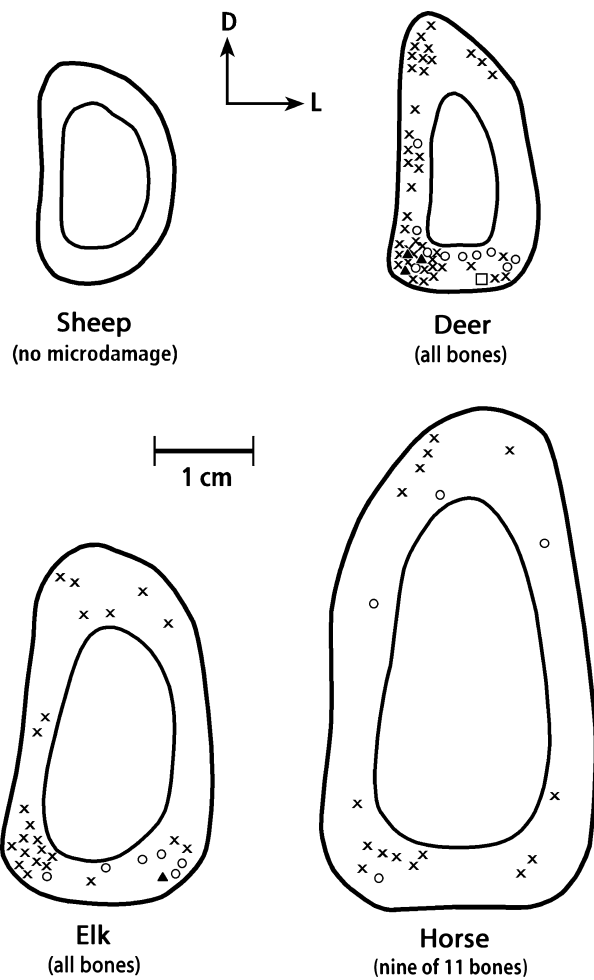
Fig. 4 Composite drawings of cross-sections of each bone with locations of each microdamage entity observed (i.e. the total amount of microdamage observed): linear (○); debonded (X); wispy (□); and diffuse (▲). The sections are from 50% of shaft length.
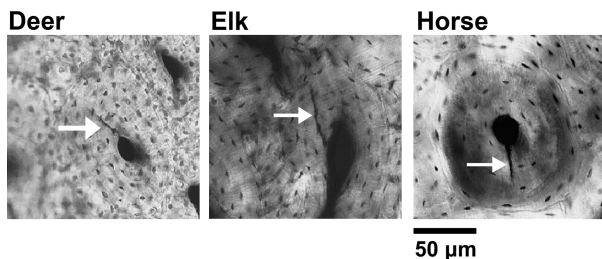
Fig. 5 Representative linear microcracks associated with secondary osteons in deer, elk and horse calcanei. The images were taken in the light microscope of the undemineralized fuchsin-stained bone specimens.

Confocal microscopy: non-linear forms of microdamage

The presence of each of the 20 linear microcracks observed in the light microscope was also confirmed using confocal microscopy (Table 1; Figs 4 and 6). Confocal microscopy also revealed a significantly greater prevalence of more subtle forms of microdamage. In Fig. 6 are representative examples of microdamage entities that were found only with the confocal microscope: debonded; wispy; and diffuse. All of these forms of microdamage were associated with cement lines of secondary osteons and are not readily discernible with light microscopy.

Additional microdamage entities were observed with the confocal microscope in deer ($n = 45$, 11 bones), elk ($n = 24$, 11 bones) and horse ($n = 15$, nine bones) calcanei. In these three species, microdamage was concentrated in the plantar cortex (Table 1; Fig. 4). No additional microdamage entities were found in the confocal microscopic analysis of sheep calcanei. In the other species, the expected regional differences in microdamage entities with strain-mode-specific morphologies were not found.

Additional (non-linear) microdamage was found both alone (i.e. independently in different sections) and in bones that had linear microcracks. For example, in the deer, four bones had linear microcracks, but all 11 bones had some type of non-linear microdamage. In the elk, two bones had linear microcracks, and all 11 bones had non-linear microdamage. In the horse, three bones had linear microcracks, and nine bones had non-linear microdamage (which included the three bones with linear microcracks). Linear microcracks were never detected without some non-linear form of microdamage somewhere else in the bone sections.

Using confocal microscopy (Z-stack images), attempts were made to measure each microdamage entity in three dimensions and to determine its orientation with respect to the long axis of the bone. In contrast to data dealing with microdamage detection, 'type' identification and length in two dimensions (see above), these three-dimensional measurements proved to be unreliable (especially for the linear microdamage entities) because of large variance in intra-observer measurements. Nevertheless, it is clear that the debonded and diffuse microdamage entities generally followed the orientation of osteonal cement lines in three dimensions. Debonded, diffuse and wispy microdamage entities did not traverse the full thickness of the specimen, being limited to 5–40 μm in the longitudinal direction. These microdamage entities also represented a zone of injury, compared with the more distinct linear microcracks.

Discussion

Compared with the other cortical locations, the plantar 'tension⁄shear' cortices of deer, elk and equine calcanei had the greatest diversity and prevalence of microdamage (percentage of all microdamage: 91% in deer; 73% in elk; and 55% in horses). These results in three of the four species seem to support our hypothesis that there would be regional differences in the prevalence of microdamage (including all sizes, lengths and types). However, absence of

Diffuse

Diffuse

Debonded

Debonded

Wispy

50 μm
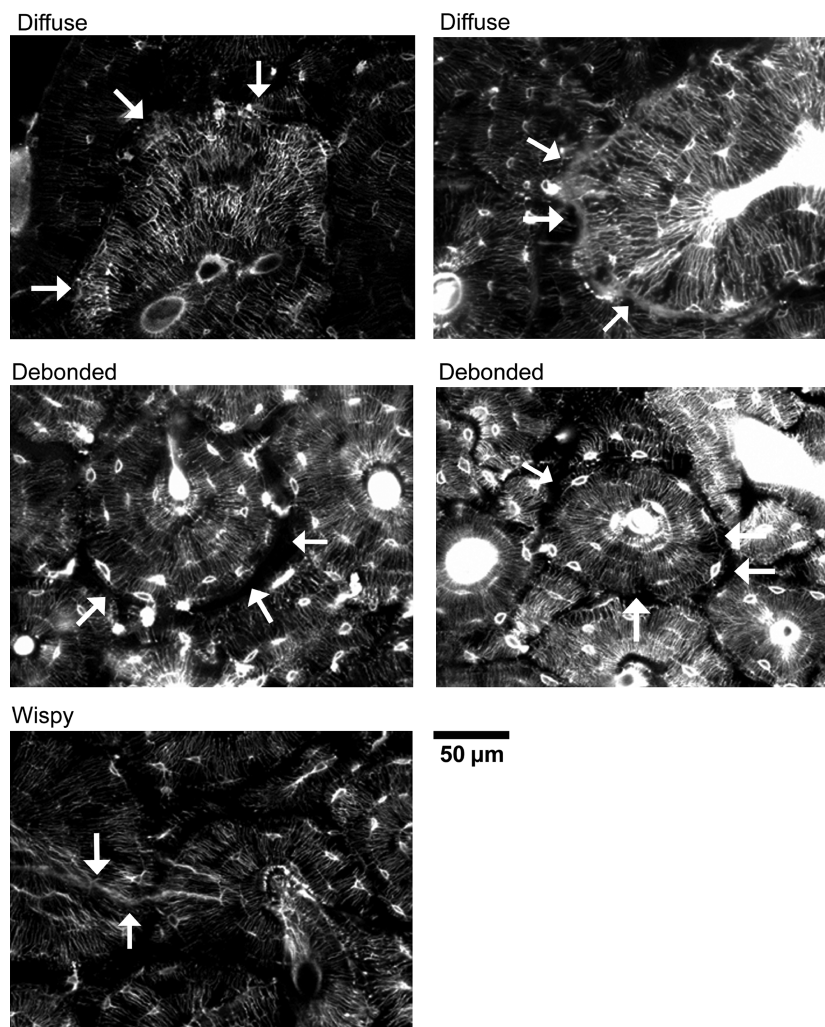
Fig. 6 Representative forms of microdamage seen in the confocal microscope: diffuse; debonded; and wispy. As shown here, the debonded damage is detected by a separation at the osteonal periphery with disruption of all canaliculi. Osteons without debonding do not show this separation, and have evidence of some canaliculi traversing across cement lines. The images are from the undemineralized fuchsin-stained bone specimens.

predicted differences in microdamage prevalence/morphology between dorsal and medial/lateral cortices of these bones, and the general absence of spatial patterns of strain-mode-specific microdamage do not support our hypotheses that these regional patterns in diversity and prevalence would be present.

Microdamage was not detected in calcanei from sheep using either confocal or light microscopy. Furthermore, microdamage prevalence in the equine calcanei was lower than the deer and elk bones. The absence, or reduced prevalence, of microdamage in these domesticated animals could reflect their generally reduced activity when compared with the wild deer and elk used in this study. Results of our previous study (Skedros et al. 1997) support this explanation in sheep calcanei by showing, in contrast to findings of the present study, a lack of significant differences in dorsal–plantar remodeling rates (estimated from differences in newly forming osteons and resorption spaces). This lack of a dorsal–plantar difference in the sheep calcanei from our previous study might reflect the fact that these animals were kept in pastures that were smaller than those that contained the sheep used in the present study. Relatively increased ambulatory activities that could occur in larger pastures might explain the significant differences in regional remodeling activity (i.e. higher in the plantar cortex) that was observed in the present study. Comparatively lower physical activity of our sheep and horses could result in strains that are not sufficient for evoking the more marked remodeling differences shown between the dorsal and plantar cortices of wild elk and deer (McMahon et al. 1995; Skedros et al. 1997). Differences in the general physical activity between individual animals at the time of specimen collection could also account for the absence or scarcity of microdamage in some bones, even in some of

the wild animals. Comparatively less intense loading, especially of the sheep calcanei, could produce peak strains that are also too low to evoke microdamage that can be detected using confocal microscopy. However, this does not rule out the possibility that more subtle damage (e.g. at the nanoscale) is responsible for activating some of the remodeling in the plantar region of the sheep calcanei and in the other bones used in the present study (Martin, 2002; Launey et al. 2010).

It must be emphasized, however, that the explanation that the lack of microdamage in sheep and horse relative to deer and elk reflects some inherent activity difference is an assumption. We know of no studies that have shown that the strain history experienced by an animal in the wild is any more or less sufficient for evoking remodeling and microdamage than what would be experienced by an animal in an enclosed paddock. To address this issue, studies are needed to determine the relative differences of the activity levels of wild vs. domesticated artiodactyls and horses.

It is also possible that the increased remodeling activity in the plantar cortices of sheep calcanei reflects a basal rate that is independent of microdamage repair. This interpretation, however, is weakened by the observation that concentrations of NREs in the plantar cortex of sheep are higher than concentrations in the plantar cortices of deer and horses – which would be expected to exhibit a basal rate plus remodeling events that are targeted at microdamage repair. It is also possible that the incidence of microdamage is similar in all but the plantar cortex. The generally higher basal remodeling rates in the sheep calcanei could be responsible for the absence of microdamage observed in these bones. Ontogenetic studies of microdamage incidence and remodeling activities (targeted and non-targeted at microdamage repair) are needed to answer these questions.

Some investigators speculate that only ∼30% or less of remodeling activity in most bones under normal conditions is targeted at microdamage repair (Burr, 2002; Parfitt, 2002). In this perspective, the remodeling activity shown in our sheep calcanei, and a large majority of remodeling activity of the other three species, might be associated with lower ambient strains in the plantar cortex – because this region is stress shielded by the plantar ligament and tendon of the superficial digital flexor muscle (Su et al. 1999). This interpretation is consistent with the non-microdamage-mediated activation of remodeling below a minimum effect strain threshold for remodeling activity as suggested by H.M. Frost (Skedros et al. 2001). Remodeling below this hypothesized threshold could be mediated by osteocyte apoptosis or by other mechanisms that can be independent of microdamage (Hughes & Petit, 2010).

An alternative explanation of higher prevalence of microdamage in plantar calcaneal cortices is that this region is more susceptible to microdamage accumulation. This might be related to the relatively deleterious habitual strain environment of this region when compared with the other regions (at least in our deer, elk and equine calcanei). In an *ex vivo* study of cortical strains on adult deer calcanei, Su et al. (1999) showed that the plantar cortex has relatively greater magnitudes of tension and shear than the other regions. The possibility that habitual tension/shear is more prone to microdamage is supported by data showing that: (i) predominant tension causes a rapid initial stiffness loss that lowers the microcrack initiation threshold compared with predominant compression or shear; (ii) mixed strain modes, similar to the 'tension/shear' environment of the plantar cortex can produce comparatively more extensive damage along shear sites, lamellar interfaces and cement lines; (iii) fatigue behavior and strength of cortical bone significantly differs in tension, compression and shear strain modes – being most notably deficient in shear and tension; and (iv) shear displacements could lead to more subtle forms of damage (e.g. injury to osteocyte dendrites) that can evoke the remodeling response by causing osteocytic apoptosis (Pattin et al. 1996; Reilly & Currey, 1999; George & Vashishth, 2005; Hazenberg et al. 2006; Cardoso et al. 2009).

Consequently, there are two conflicting hypotheses at work here: (i) greater metabolic-related remodeling in the plantar cortex due to a low strain environment where material resorption might not be so detrimental; and (ii) greater remodeling due to greater shear strains and damage accumulation. This reflects the complexity of the relationships between microdamage formation/propagation, microstructure and mechanical properties. The increased remodeling activity of the plantar cortices of the four species examined not only increases osteonal porosity and osteon population density, but also decreases the bulk tissue mineralization by decreasing the mean age of the osteons. While this would appear to jeopardize the material's integrity by reducing elastic modulus and increasing fatigue microdamage, there are data showing that this is well compensated by the toughening effect of the younger osteons (Kennedy et al. 2008), which are highly concentrated in the plantar cortex.

Alternatively, it may be that the lack of microdamage in the sheep calcanei reflects allometric relationships between cross-sectional and second moment of area parameters, and physiological cross-sectional areas of the gastrocnemius muscle, which result in relatively lower forces on the sheep calcaneus with respect to body size. In other words, for example, the deer calcanei (which have the overall highest concentration of microdamage), may have relatively greater muscle cross-sectional area for their size than do sheep, and hence relatively greater forces on the calcaneus relative to body mass and/or geometrical/structural properties of the bones. Further study is warranted of these possible allometric relationships among the four species examined in this study.

Comparisons with data from human metatarsals

Using only light microscopy, Donahue et al. (2000) examined potential *in vivo* strain-mode-specific microdamage in the second and fifth metatarsals of 15 human feet ranging in age from 41–86 years (mean 72 years). These investigators reported that the density of linear microdamage ranged from 0.43 mm^{-2} (standard deviation: 0.41) in the plantar–lateral quadrant to 0.26 mm^{-2} (SD: 0.26) in the dorsal–lateral quadrant (lowest *P*-value for quadrant comparisons = 0.14). If their sample size was insufficient for detecting a significant difference, then it would be important to re-evaluate this comparison because this statistical tendency reflects a potential strain-mode-related effect as revealed by *ex vivo* strain gage analyses (i.e. habitual compression in the dorsal–lateral cortex and habitual tension in the plantar–lateral cortex; Goodwin & Sharkey, 2002).

Microdamage and cortical 'toughening'

Our results suggest that the prevalence of non-linear microdamage entities was fourfold greater than linear microdamage. This difference might reflect the preferential repair of linear microcracks because they may be the most severe manifestations of fatigue microdamage. This is because linear microcracks are believed to be able to propagate and coalesce to cause stress fractures (Martin et al. 1998), and this behavior is more likely with larger linear microcracks (O'Brien et al. 2005; Martin, 2007). Studies using the rat ulna model have shown that linear microcracks are preferentially repaired over other kinds of damage (Bentolila et al. 1998; Herman et al. 2010). We know of no studies that have shown that this also occurs in mammals that have the natural capacity for extensive osteonal remodeling. Until these studies are done, equal consideration must be given to the possibility that linear microcracks may simply occur much less commonly than other kinds of damage and that is why they are less abundant.

It has been suggested that the remarkable differences in material organization of the dorsal, plantar, medial and lateral cortices of sheep and deer calcanei that emerge during normal development represent non-uniform remodeling activities that differentially 'toughen' the material for local differences in ambient strain characteristics (Skedros et al. 2004, 2006a, 2007; Fig. 7). In the perspective of our data showing the absence of regional heterogeneity in microdamage morphology, the remarkable material/remodeling heterogeneity among the main cortical regions could be adaptations that avoid potentially deleterious amounts of strain-mode-specific and non-specific microdamage, especially longer linear microcracks. Consequently, the emergence of regionally 'specific' material adaptations (including differences in remodeling activity, predominant collagen fiber orientation and osteonal morphotypes) during normal development may restrict the subsequent

formation of these forms of microdamage. We speculate that these material variations minimize deleterious increases and regional disparities in microdamage accumulation and/or propagation even though the bone is subject to a highly non-uniform strain distribution. However, the production of non-specific microdamage (including the presumed nanoscale damage) that still occurs is beneficial because it can dissipate energy that could otherwise lead to fracture of the bone (Reilly et al. 1997; Donahue et al. 2000; Launey et al. 2010).

A limitation of the present investigation is that there are only two studies that have measured *in vivo* strains on calcanei from any of the species used herein, and both were in the sheep calcaneus (Lanyon, 1973, 1974). These studies,
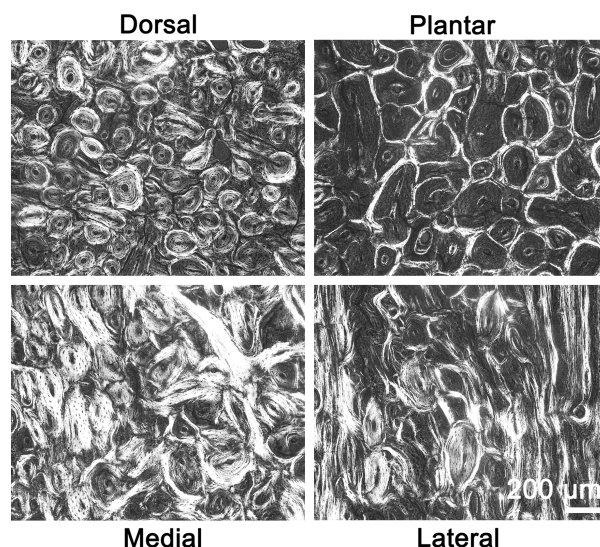
Fig. 7 Circularly polarized images from the same population of adult sheep used in the present study. The images are from a previous study (Skedros et al. 2007), and they show regional variations in secondary osteon population density and morphology (including cross-sectional size, shape and patterns of predominant collagen orientation). The dorsal 'compression' cortex has prevalent 'bright' and 'alternating' osteons (i.e. with patterns of alternating birefringence). 'Hoop'/parallel-fibered osteons seen in the plantar cortex contain relatively more longitudinal collagen and correspond to a history of tension loads. These osteonal characteristics can modify microdamage formation, propagation and arrest in their respective strain environments (Hiller et al. 2003; Gibson et al. 2006). Important hypotheses are: (i) regional differences in the morphology and/or prevalence of specific microdamage entities evoke differences in remodeling activities that ultimately produce the highly adapted microstructural heterogeneity between regions of the same cross-section; and (ii) this heterogeneity is primarily aimed at optimizing regional toughness for variations in predominant strain mode/magnitude. The specimens were embedded undemineralized and unstained in polymethyl methacrylate, sectioned transversely at 70% length (Fig. 2), and ultramilled to 100 μm. The images were taken at the same magnification and illumination; in all images dorsal is toward the top edge of the image and lateral is toward the right edge of the image. The scale bar represents 200 μm.

however, did not include extreme loading conditions (e.g. running and darting), and did not attempt to place a strain gage on the plantar cortex (i.e. beneath the plantar ligament). These studies also only measured strains on the lateral cortex. Other studies that less directly support the relatively simple load history described in the present study include: (i) an *ex vivo* study of deer calcanei that used up to seven stacked-rosette gages on the same bone, normal and extreme load conditions, and strain gages on the plantar cortex (Su et al. 1999); and (ii) biomechanical analyses of horse calcanei that did not use *in vivo* strain data (Badoux, 1987; Vander Sloten & Van der Perre, 1989). However, the deer calcaneus data were obtained from a fixed limb position. Lanyon's data for the lateral sheep calcaneus showed that peak shear strains on the lateral surface do not occur at midstance, which is the time point modeled in Su et al. (1999). Clearly, additional *in vivo* studies are needed to better characterize the strain distribution of the calcanei from the wild and domesticated animals used herein in order to more rigorously define the limitations of considering them as relatively simply loaded cantilevered beams.

In summary, although targeted remodeling may have removed evidence of the expected regional differences in strain-mode-specific microdamage in the bones that exhibited microdamage (deer, elk, horse), the highest overall concentrations occurred in the plantar cortex. This might reflect increased susceptibility of non-specific microdamage in habitual tension∕shear and∕or could be related to relatively greater physical activity of the deer, elk and horses relative to that of sheep. Absence of differences in microdamage prevalence∕morphology between dorsal, medial and lateral cortices of these bones might also reflect the prior remodeling activity that subsequently reduces the likelihood of incurring potentially deleterious concentrations of strain-mode-specific microdamage. By contrast, it is possible that either the generally higher basal remodeling rates in the sheep calcanei could be responsible for the absence of microdamage observed in these bones, or these bones are from animals in smaller pastures that preclude the physical activity required for producing microdamage. Additional biomechanical and ontogenetic studies of these models are needed to explore the putative relationships between naturally occurring microdamage, non-uniform strain distribution, and the developmental emergence and subsequent maintenance of their remarkable regional material heterogeneity. It is likely that the mechanistic bases of these relationships are broadly applicable to all limb bones that undergo osteonal remodeling during their normal development.

Acknowledgements

Author contributions

Disclosures

References

Badoux DM (1987) Some biomechanical aspects of the structure of the equine tarsus. *Anat Anz* **164**, 53–61.

Banks WJ Jr, Epling GP, Kainer RA, et al. (1968) I. Morphological and morphometric changes in the costal compacta during the antler growth cycle. *Anat Rec* **162**, 387–398.

Bentolila V, Boyce TM, Fyhrie DP, et al. (1998) Intracortical remodeling in adult rat long bones after fatigue loading. *Bone* **23**, 275–281.

Biewener AA, Bertram JEA (1993) Mechanical loading and bone growth *in vivo*. In:*Bone, Volume 7, Bone Growth-B* (ed. Hall BK), pp. 1–36, Boca Raton, FL: CRC Press.

Boyce TM, Fyhrie DP, Glotkowski MC, et al. (1998) Damage type and strain mode associations in human compact bone bending fatigue. *J Orthop Res* **16**, 322–329.

Burr DB (2002) Targeted and nontargeted remodeling. *Bone* **30**, 2–4.

Burr DB, Hooser M (1995) Alterations to the en bloc basic fuchsin staining protocol for the demonstration of microdamage produced in vivo. *Bone* **17**, 431–433.

Burr DB, Stafford T (1990) Validity of the bulk-staining technique to separate artifactual from *in vivo* bone microdamage. *Clin Orthop* **260**, 305–308.

Cardoso L, Herman BC, Verborgt O, et al. (2009) Osteocyte apoptosis controls activation of intracortical resorption in response to bone fatigue. *J Bone Miner Res* **24**, 597–605.

Colopy SA, Benz-Dean J, Barrett JG, et al. (2004) Response of the osteocyte syncytium adjacent to and distant from linear microcracks during adaptation to cyclic fatigue loading. *Bone* **35**, 881–891.

Currey JD (2002) *Bones: Structure and Mechanics*. Princeton, NJ: Princeton University Press.

Da Costa Gómez TM, Barrett JG, Sample SJ, et al. (2005) Up-regulation of site-specific remodeling without accumulation of microcracking and loss of osteocytes. *Bone* **37**, 16–24.

Diab T, Vashishth D (2007) Morphology, localization and accumulation of *in vivo* microdamage in human cortical bone. *Bone* **40**, 612–618.

Donahue SW, Galley SA (2006) Microdamage in bone: implications for fracture, repair, remodeling, and adaptation. *Crit Rev Biomed Eng* **34**, 215–271.

Donahue SW, Sharkey NA, Modanlou KA, et al. (2000) Bone strain and microcracks at stress fracture sites in human metatarsals. *Bone* **27**, 827–833.

Ebacher V, Tang C, McKay H, et al. (2007) Strain redistribution and cracking behavior of human bone during bending. *Bone* **40**, 1265–1275.

Fritton SP, Rubin CT (2001) *In vivo* measurement of bone deformations using strain gauges. In:*Bone Biomechanics Handbook* (ed. Cowin SC). Boca Raton: CRC Press.

Frost HM (1960) Presence of microscopic cracks in vivo in bone. *Henry Ford Hosp Med Bull* **8**, 25–35.

George WT, Vashishth D (2005) Damage mechanisms and failure modes of cortical bone under components of physiological loading. *J Orthop Res* **23**, 1047–1053.

Gibson VA, Stover SM, Gibeling JC, et al. (2006) Osteonal effects on elastic modulus and fatigue life in equine bone. *J Biomech* **39**, 217–225.

Goodwin KJ, Sharkey NA (2002) Material properties of interstitial lamellae reflect local strain environments. *J Orthop Res* **20**, 600–606.

Hazenberg JG, Freeley M, Foran E, et al. (2006) Microdamage: a cell transducing mechanism based on ruptured osteocyte processes. *J Biomech* **39**, 2096–2103.

Herman BC, Cardoso L, Majeska RJ, et al. (2010) Activation of bone remodeling after fatigue: differential response to linear microcracks and diffuse damage. *Bone* **47**, 766–772.

Hiller LP, Stover SM, Gibson VA, et al. (2003) Osteon pullout in the equine third metacarpal bone: effects of *ex vivo* fatigue. *J Orthop Res* **21**, 481–488.

Hillman JR, Davis RW, Abdelbaki YZ (1973) Cyclic bone remodeling in deer. *Calcif Tissue Res* **12**, 323–330.

Hughes JM, Petit MA (2010) Biological underpinnings of Frost's mechanostat thresholds: the important role of osteocytes. *J Musculoskelet Neuronal Interact* **10**, 128–135.

Kennedy OD, Brennan O, Mauer P, et al. (2008) The effects of increased intracortical remodeling on microcrack behaviour in compact bone. *Bone* **43**, 889–893.

Lanyon LE (1973) Analysis of surface bone strain in the calcaneus of sheep during normal locomotion. Strain analysis of the calcaneus. *J Biomech* **6**, 41–49.

Lanyon LE (1974) Experimental support for the trajectorial theory of bone structure. *J Bone Joint Surg* **56B**, 160–166.

Lanyon LE, Magee PT, Baggott DG (1979) The relationship of functional stress and strain to the processes of bone remodeling: an experimental study on the sheep radius. *J Biomech* **12**, 593–600.

Launey ME, Buehler MJ, Ritchie RO (2010) On the mechanistic origins of toughness in bone. *Annu Rev Mater Res* **40**, 25–53.

Lee TC, Myers ER, Hayes WC (1998) Fluorescence-aided detection of microdamage in compact bone. *J Anat* **193**(Pt 2), 179–184.

Lieberman DE, Pearson OM, Polk JD, et al. (2003) Optimization of bone growth and remodeling in response to loading in tapered mammalian limbs. *J Exp Biol* **206**, 3125–3138.

Martin RB (2002) Is all cortical bone remodeling initiated by microdamage? *Bone* **30**, 8–13.

Martin RB (2007) The importance of mechanical loading in bone biology and medicine. *J Musculoskelet Neuronal Interact* **7**, 48–53.

Martin RB, Burr DB, Sharkey NA (1998) *Skeletal Tissue Mechanics*. New York, NY: Springer.

McMahon JM, Boyde A, Bromage TG (1995) Pattern of collagen fiber orientation in the ovine calcaneal shaft and its relation to locomotor-induced strain. *Anat Rec* **242**, 147–158.

Moreno CA, Main RP, Biewener AA (2008) Variability in forelimb bone strains during non-steady locomotor activities in goats. *J Exp Biol* **211**, 1148–1162.

Norman TL, Wang Z (1997) Microdamage of human cortical bone: incidence and morphology in long bones. *Bone* **20**, 375–379.

O'Brien FJ, Taylor D, Lee TC (2003) Microcrack accumulation at different intervals during fatigue testing of compact bone. *J Biomechanics* **36**, 973–980.

O'Brien F, Taylor D, Lee TC (2005) The effect of bone microstructure on the initiation and growth of microcracks. *J Orthop Res* **23**, 475–480.

Parfitt AM (2002) Targeted and nontargeted bone remodeling: relationship to basic multicellular unit origination and progression. *Bone* **30**, 5–7.

Pattin CA, Caler WE, Carter DR (1996) Cyclic mechanical property degradation during fatigue loading of cortical bone. *J Biomech* **29**, 69–79.

Reilly GC (2000) Observations of microdamage around osteocyte lacunae in bone. *J Biomech* **33**, 1131–1134.

Reilly GC, Currey JD (1999) The development of microcracking and failure in bone depends on the loading mode to which it is adapted. *J Exp Biol* **202**, 543–552.

Reilly GC, Currey JD, Goodship AE (1997) Exercise of young thoroughbred horses increases impact strength of the third metacarpal bone. *J Orthop Res* **15**, 862–868.

Robling AG, Castillo AB, Turner CH (2006) Biomechanical and molecular regulation of bone remodeling. *Annu Rev Biomed Eng* **8**, 455–498.

Skedros JG (2011) Interpreting load history in limb-bone diaphyses: important considerations and their biomechanical foundations. In:*Bone Histology: an Anthropological Perspective* (eds Crowder C, Stout S), pp. 423. Boca Raton, Florida: CRC Press.

Skedros JG, Mason MW, Bloebaum RD (1994) Differences in osteonal micromorphology between tensile and compressive cortices of a bending skeletal system: indications of potential strain-specific differences in bone microstructure. *Anat Rec* **239**, 405–413.

Skedros JG, Su SC, Bloebaum RD (1997) Biomechanical implications of mineral content and microstructural variations in cortical bone of horse, elk, and sheep calcanei. *Anat Rec* **249**, 297–316.

Skedros JG, Mason MW, Bloebaum RD (2001) Modeling and remodeling in a developing artiodactyl calcaneus: a model for evaluating Frost's mechanostat hypothesis and its corollaries. *Anat Rec* **263**, 167–185.

Skedros JG, Sybrowsky CL, Parry TR, et al. (2003) Regional differences in cortical bone organization and microdamage prevalence in Rocky Mountain mule deer. *Anat Rec* **274A**, 837–850.

Skedros JG, Hunt KJ, Bloebaum RD (2004) Relationships of loading history and structural and material characteristics of bone: development of the mule deer calcaneus. *J Morphol* **259**, 281–307.

Skedros JG, Dayton MR, Sybrowsky CL, et al. (2006a) The influence of collagen fiber orientation and other histocompositional characteristics on the mechanical properties of equine cortical bone. *J Exp Biol* **209**, 3025–3042.

Skedros JG, Sorenson SM, Takano Y, et al. (2006b) Dissociation of mineral and collagen orientations may differentially adapt compact bone for regional loading environments: results from acoustic velocity measurements in deer calcanei. *Bone* **39**, 143–151.

Skedros JG, Sorenson SM, Hunt KJ, et al. (2007) Ontogenetic structural and material variations in ovine calcanei: a model for interpreting bone adaptation. *Anat Rec* **290**, 284–300.

Skedros JG, Mendenhall SD, Kiser CJ, et al. (2009) Interpreting cortical bone adaptation and load history by quantifying osteon morphotypes in circularly polarized light images. *Bone* **44**, 392–403.

Sokal RR, Rohlf FJ (1995) *Biometry. The Principles and Practice of Statistics in Biological Research*, 3rd edn. New York: W.H. Freeman.

Su SC (1998) Microstructure and mineral content correlations to strain parameters in cortical bone of the artiodactyl calcaneus. In:*Department of Bioengineering* (Masters Thesis), pp. 64. Salt Lake City, UT: University of Utah.

Su SC, Skedros JG, Bachus KN, et al. (1999) Loading conditions and cortical bone construction of an artiodactyl calcaneus. *J Exp Biol* **202**(Pt 22), 3239–3254.

Taylor D, Lee TC (1998) Measuring the shape and size of microcracks in bone. *J Biomech* **31**, 1177–1180.

Vander Sloten J, Van der Perre G (1989) Trabecular structure compared to stress trajectories in the proximal femur and the calcaneus. *J Biomed Eng* **11**, 203–208.

Vashishth D (2004) Rising crack-growth-resistance behavior in cortical bone: implications for toughness measurements. *J Biomech* **37**, 943–946.

Vashishth D, Koontz J, Qiu SJ, et al. (2000) In vivo diffuse damage in human vertebral trabecular bone. *Bone* **26**, 147–152.

Wang X, Niebur GL (2006) Microdamage propagation in trabecular bone due to changes in loading mode. *J Biomech* **39**, 781–790.

Zioupos P, Currey JD (1994) The extent of microcracking and the morphology of microcracks in damaged bone. *J Mater Sci* **29**, 978–986.